SF2A 2014
J. Ballet, F. Bournaud, F. Martins, R. Monier and C. Reylé (eds)

THE VIOLENT YOUTH OF BRIGHT AND MASSIVE CLUSTER GALAXIES AND THEIR MATURATION OVER 7 BILLION YEARS

B. Ascaso[1], B. Lemaux[2], L. M. Lubin[3], R.R. Gal[4], D.D. Kocevski[5], N. Rumbaugh[3] and G. Squires[6]

Abstract. In this talk, I will present recent research on the formation and evolution mechanisms of the brightest cluster galaxies (BCGs) over cosmic time. At high redshift (z∼0.9) we selected BCGs and most massive cluster galaxies (MMCGs) from the Cl1604 supercluster and compared to low-redshift (z∼0.1) counterparts drawn from the MCXC meta-catalog and supplemented by SDSS imaging and spectroscopy. We observed striking differences in the morphological, color, spectral, and stellar mass properties of the BCGs/MMCGs in the two samples. High-redshift BCGs/MMCGs were, in many cases, star-forming, late-type galaxies, with blue broadband colors, properties largely absent amongst the low-redshift BCGs/MMCGs. The stellar mass of BCGs was found to increase by an average factor of 2.51±0.71 from z∼0.9 to z∼0.1. Through this and other comparisons we conclude that a combination of major merging (mainly wet or mixed) and in situ star formation are the main mechanisms which build stellar mass in BCGs/MMCGs. The stellar mass growth of the BCGs/MMCGs also appears to grow in lockstep with both the stellar baryonic and total mass of the cluster. Additionally, BCGs/MMCGs were found to grow in size, on average, a factor of ∼3 while their average Sérsic index increased by ∼0.45 from z∼0.9 to z∼0.1, also supporting a scenario involving major merging, though some adiabatic expansion is required. These observational results are compared to both models and simulations to further explore the implications on processes which shape and evolve BCGs/MMCGs over the past ∼7 Gyr.

Keywords: techniques: photometric, techniques: spectroscopic, galaxies: clusters: general, galaxies: elliptical and lenticular, cD, galaxies: evolution, galaxies: formation

1 Data

In this work, we consider the Brightest Cluster Galaxy (BCG) and Most Massive Cluster Galaxy (MMCG) of the $z \sim 0.9$ Cl1604 supercluster, which contains clusters and groups that span a wide range in halo mass, and a comparison sample of comparable clusters at low-redshift ($z \sim 0.1$) observed as part of the Sloan Digital Sky Survey (SDSS).

1.1 *The Cl1604 supercluster at* $z \sim 0.9$

The Cl1604 supercluster, located at $z \sim 0.9$, is one of the most well-characterized superclusters in the high-redshift universe and it has exhaustively observed as part of the Observations of Redshift Evolution in Large Scale Environment survey (ORELSE; Lubin et al. 2009). The supercluster consists of three galaxy clusters and five groups (Gal et al. 2008).

There exists a vast number of observations for this supercluster (see Lemaux et al. (2012); Ascaso et al. (2014) and references herein). In this work, we have using the fact that the systems have been spectroscopically sampled to a completeness limit of $M_g = -20.35$ and, additionally, they have associated deep F606W/F814W HST ACS imaging down to 27.2 and 26.8 mags for point sources in the shallowest regions.

[1] Observatoire de Paris, 77 Denfert Rochereau, 75014, Paris, France
[2] Laboratoire dAstrophysique de Marseille, 38 rue F. Joliot-Curie, 13388, Marseille, France
[3] University of California Davis, One Shields Avenue, 95616, Davis, CA, USA
[4] Institute for Astronomy, University of Hawaii, 2680 Woodlawn Drive, Honolulu, HI 96822, USA
[5] University of Kentucky, 505 Rose Street, Lexington, KY 40506, USA
[6] Spitzer Science Center, California Institute of Technology, M/S 220-6, 1200 E. California Blvd, Pasadena, CA 91125, USA

For each cluster or group, we select the BCG as the member galaxy with the brightest $F814W$ magnitude within $r_{\rm proj} < 1h_{70}^{-1}$ Mpc of the luminosity-weighted cluster/group center. We also selected the MMCG in a nearly identical manner as the BCGs, with the exception that the stellar mass derived through SED-fitting process or through the K-band imaging was used in place of the $F814W$ magnitude. In all cases galaxies with stellar masses within 1σ of that of the galaxy with the highest measured mass were also selected and our analysis was repeated for each potential MMCG (setting a maximum of three MMCG "candidates" for each cluster/group). The final sample of 17 galaxies consisted of eight BCGs and nine MMCGs.

1.2 MCXC clusters at $z \sim 0.1$

We drew a sample of low-redshift clusters from the Meta-Catalog of the compiled properties of X-ray detected galaxy Clusters (MCXC; Piffaretti et al. 2011). This catalog contains a large number of galaxy clusters with well-defined and homogeneously measured X-Ray luminosities. Moreover, it overlaps with the SDSS, allowing us to access to an enormous dataset of well-calibrated and internally consistent multiwavelength imaging and spectroscopy.

We selected a sample of galaxy clusters from the MCXC catalog by cross correlating it with the SDSS DR8 public database. For those clusters which fell within the SDSS footprint we required that any potential comparison cluster have *i*) imaging in the g' band to sufficient depth to make valid morphological comparisons ($\sim$ 23.5 mag/arcsec^2), *ii*) sufficient photometry to estimate stellar masses (i.e., measured magnitudes in all SDSS bands), *iii*) spectroscopy of at least 80% of potential member galaxies brighter than $M_{g'} = -20.35$ that lie within a projected distance of $1h_{70}^{-1}$ Mpc from the cluster center, and *iv*) spectroscopy of the 10 brightest objects in the g' band within a projected distance of $1h_{70}^{-1}$ Mpc from the cluster center as defined by the MCXC X-Ray centroid. Imposing these criteria resulted in a sample of 100 low-redshift clusters out of the 1743 clusters contained within the MCXC catalog. Finally, we excluded those clusters with questionable color-magnitude diagram or velocity dispersion measurement obtaining a final sample of 81 clusters with a median redshift of $\langle z \rangle = 0.08$ and a redshift range of $z = 0.02 - 0.21$.

The BCG and MMCG for each cluster was selected in a manner identical to that of the Cl1604 BCGs, with the selection being performed in the g' band (see Ascaso et al. 2014 for further details). Only 13 had a BCG that differed from the MMCG.

2 Results

We investigated the evolution of color, morphological, stellar mass, and spectral properties of BCGs/MMCGs over the past $\sim$ 7 Gyr. Our results are as follows.

- *Color and luminosity evolution:* A large fraction ($\sim$ 35%) of the combined Cl1604 BCG/MMCG sample were observed with colors blueward of the red sequence for its parent cluster or group. In contrast, only a small fraction ($\sim$ 2%) of the BCGs/MMCGs at low redshift were observed to be similarly offset of the red sequence. The gap in magnitude between the BCG and the next brightest cluster/group galaxy in the average Cl1604 cluster/group was found to be less than half that of the average MCXC cluster.

- *Morphology evolution:* Exactly half of the Cl1604 BCG sample were galaxies classified with late-type morphologies and a large fraction ($\sim$ 40%) of had signs of interaction. In contrast, only 2.5% the BCGs at low redshift were classified as late-type and the fraction of those undergoing interactions was less than half of that of the Cl1604 sample. In addition, the Cl1604 BCGs were observed in some stage of a merging event greater than five times more frequently than the low-z BCGs. These numbers did not change appreciably when the MMCGs of the two samples were considered.

- *Spectral evolution:* A majority ($\sim$53%) of the combined Cl1604 BCG/MMCG sample show significant ongoing star formation. In contrast, only a small fraction $\sim$ 4% of the MCXC BCGs/MMCGs were observed with ongoing star formation. From a stacked spectrum of galaxies, the average star formation rate of the Cl1604 BCGs/MMCGs was found to be $\langle SFR \rangle = 10.5 \pm 0.5\ \mathcal{M}_\odot\ {\rm yr}^{-1}$. This value is in stark contrast with the average SFR of the MCXC-SDSS BCG/MMCG, which was consistent with zero. In addition, strong Balmer absorption features and weak features associated with older stellar populations were observed in the Cl1604 BCG/MMCG stacked spectrum, which indicated a considerably younger mean luminosity-weighted stellar age as compared to the MCXC/SDSS sample. Even those

Cl1604 BCGs/MMCGs considered passive (SSFR $< 10^{11} yr^{-1}$) showed signs of a moderately young stellar population.

- *Stellar mass evolution:* The average $z \sim 0.9$ Cl1604 BCG was observed to be deficient in stellar mass by a factor of 2.51±0.71 relative to a (cluster total mass) matched sample of $z \sim 0.1$ MCXC BCGs. The average MMCG in Cl1604 was found to be deficient in stellar mass by a factor of 1.78±0.45 relative to the MMCGs same matched low-redshift sample. Surprisingly, this growth factor is consistent with both the increase in total mass and increase of total stellar baryonic mass of the clusters over the same redshift interval. This result strongly suggested that the growth of the stellar mass of a BCG/MMCG is intimately linked with both the total stellar (contained in galaxies) and dark matter growth of the clusters.

- *Radial distribution of stellar mass:* A comparison was made between the stellar mass surrounding the BCGs/MMCGs at low and high redshift in the form of companion galaxies. A marked increase of stellar mass at low (projected) radii $R_{\rm proj} < 0.3R_{vir}$ was observed surrounding the Cl1604 BCGs/MMCGs relative to the MCXC BCGs/MMCGs (see Fig. 1). Merging timescales were calculated for all companion galaxies to the Cl1604 BCGs/MMCGs that had the possibility of merging within ≤7 Gyr. Of the 15 merger candidates surrounding the Cl1604 BCGs/MMCGs with small enough merging timescales, 14 would result in a major merging event (≤4:1 mass ratio). These potential merging events are primarily comprised of the mixed or wet variety. From these merging events alone, the average Cl1604 BCG will increase in stellar mass by a factor of 2.23±0.73 and the average Cl1604 MMCG by a factor of 1.35±0.31 under the assumption of 100% retention of stellar matter.

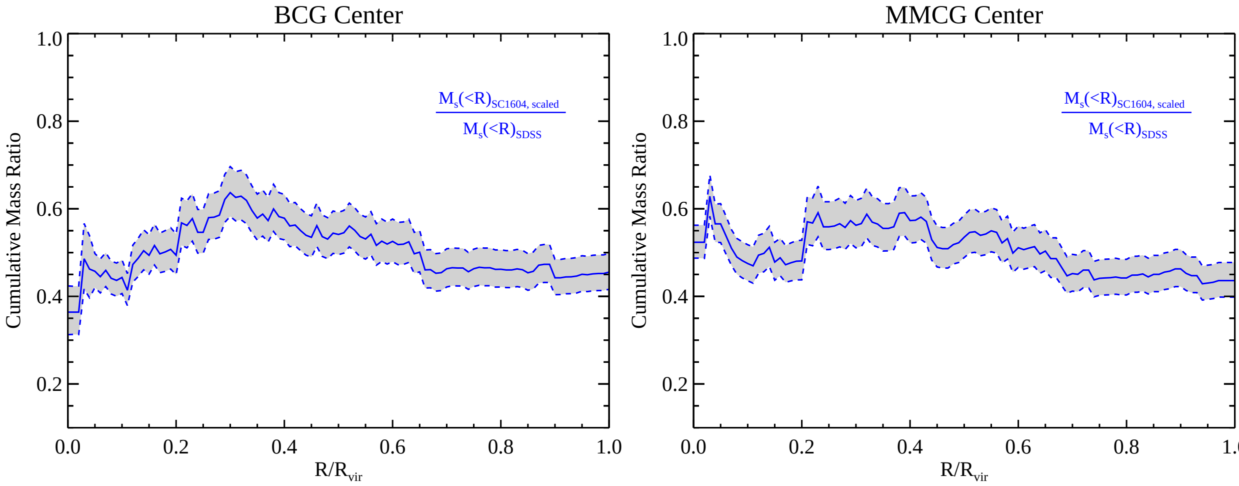

Fig. 1. The ratio of the Cl1604 to the MCXC radial stellar mass cumulative distribution using the BCG (left panel) and the MMCG (right panel) as centers. The blue line shows the average ratio between the the cumulative stellar mass distribution in the average Cl1604 cluster/group and that of the average MCXC cluster in the comparison sample. The gray shaded region denotes the sample variance at each radius. The projected radial distance of members of all clusters and groups are normalized by the virial radii of their parent structures. An increase in the ratio in either panel indicates an excess in stellar mass surrounding the average BCG/MMCG in the high-redshift clusters and groups relative to that surrounding the average low-redshift BCG/MMCG. The average BCG at high redshift shows a decided excess of stellar mass at a relatively low (normalized) radius increasing steadily out to $R \sim 0.3R_{vir}$. The average MMCG at high redshift also shows a sharp excess of stellar mass in its immediate surroundings relative to the average low-redshift MMCG, but only at very small (normalized) radius ($R < 0.05R_{vir}$). This excess indicates the presence of extremely massive companions of the high-redshift MMCGs that are not present at low redshift.

- *Structural parameter evolution*: By fitting the surface brightness profiles of all BCGs/MMCGs in both the high- and low-redshift samples to a single Sérsic profile, we found an increase of a factor of ~ 3 of the size (r_e) of BCGs/MMCGs over the past ~ 7 Gyr. The factor of this size increase was invariant with respect to which low-redshift sample we chose to compare the Cl1604 BCGs/MMCGs to. An increase in the average Sérsic index was also measured over the same redshift range, though its evolution was milder, with an observed increase of $n(z = 0) - n(z) \sim 0.5$.

3 Conclusions

From our observational data alone, we strongly favored a scenario in which BCGs/MMCGs grow through a combination of *in situ* star formation and major merging events, the latter likely causing subsequent increases in star formation activity. Though we could not completely rule out the involvement of minor mergers in building up at least a small fraction of the stellar mass of the BCGs/MMCGs over the past ~ 7 Gyr, the aforementioned scenario is wholly consistent with all of the results in this study. These observational results were then compared to a variety of hydrodynamical simulations (Hopkins et al. 2010) and semi-analytic models (De Lucia & Blaizot 2007). Through these comparisons we found that the observed prevalence of (potentially) impending major merging events amongst the Cl1604 BCGs/MMCGs was sufficient to explain the evolution in the size of BCGs/MMCGs from $z \sim 0.9$ to $z \sim 0.1$. However, the observed evolution in the average Sérsic index was not as dramatic as that predicted from a large number of major merging events. In order to explain this mild evolution, we appealed to adiabatic expansion, a process which will serve to soften the evolution of Sérsic indices of galaxies and a process which naturally follows from the ignition of an AGN as a result of a wet or mixed merging event.

This study represents one of the most comprehensive studies of the evolution of BCGs/MMCGs over cosmic time to date in terms of the sheer amount of spectroscopic and imaging data utilized for the galaxy populations of clusters at both high and low redshift. From this study we were able to draw a definitive picture of the evolution of BCGs/MMCGs in the Cl1604 supercluster. However, the sample of BCGs/MMCGs used here, especially at high redshift, remains somewhat small, and given the large amount of intrinsic variance amongst galaxy cluster populations observed at all redshifts, it is not entirely clear how applicable this picture is to the evolution of an "average" BCG over the past ~ 7 Gyr. It is encouraging that our results, or at least those which can be directly compared, show broad agreement with similar samples of BCGs taken from other surveys. However, future work remains to utilize data from the ~ 50 high-redshift clusters and groups of the full ORELSE sample, as well as datasets available from other high-redshift cluster surveys (e.g., EDisCS, GCLASS), to determine if the mode of evolution observed here amongst the Cl1604 BCGs/MMCGs is fully representative of that of typical BCGs observed across the universe.

All the results and techniques developed in this work can be found in Ascaso et al. (2014).

References

Ascaso, B., Lemaux, B. C., Lubin, L. M., et al. 2014, MNRAS, 442, 589

De Lucia, G. & Blaizot, J. 2007, MNRAS, 375, 2

Gal, R. R., Lemaux, B. C., Lubin, L. M., Kocevski, D., & Squires, G. K. 2008, ApJ, 684, 933

Hopkins, P. F., Bundy, K., Hernquist, L., Wuyts, S., & Cox, T. J. 2010, MNRAS, 401, 1099

Lemaux, B. C., Gal, R. R., Lubin, L. M., et al. 2012, ApJ, 745, 106

Lubin, L. M., Gal, R. R., Lemaux, B. C., Kocevski, D. D., & Squires, G. K. 2009, AJ, 137, 4867

Piffaretti, R., Arnaud, M., Pratt, G. W., Pointecouteau, E., & Melin, J.-B. 2011, A&A, 534, A109